Supporting Information

ZnO Nanorods/ZnS·(1, 6-hexanediamine)$_{0.5}$ Hybrid Nanoplates Hierarchical Heteroarchitecture with Improved Electrochemical Catalytic Properties for Hydrazine

Zhengcui Wu*, Yaqin Wu, Tonghui Pei, Huan Wang and Baoyou Geng*

Anhui Key Laboratory of Molecule-Based Materials, The Key Laboratory of Functional Molecular Solids, Ministry of Education, College of Chemistry and Materials Science, Anhui Normal University, Wuhu 241000, People's Republic of China

*E-mail: zhengcui@mail.ahnu.edu.cn, bygeng@mail.ahnu.edu.cn.

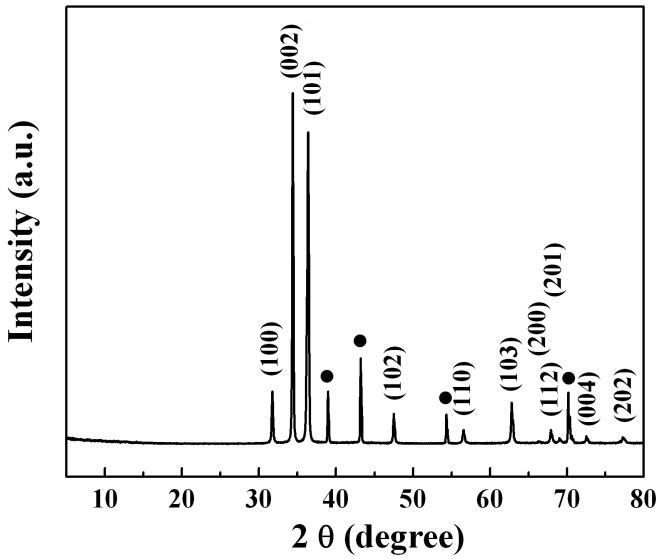

Fig. S1 The XRD pattern of ZnO-NRs on the zinc substrate.

The result demonstrates that the ZnO-NRs are well-crystallized and the diffraction peaks could be perfectly indexed to the hexagonal phase ZnO (JCPDS No. 79-0206). Moreover, four weak peaks with black dots, attributed to the characteristic peaks of zinc foil, can also be observed in this pattern, confirming that ZnO nanostructures are developed directly on the zinc substrate. No impurity peaks from other phases were detected, indicating the high purity of the product.

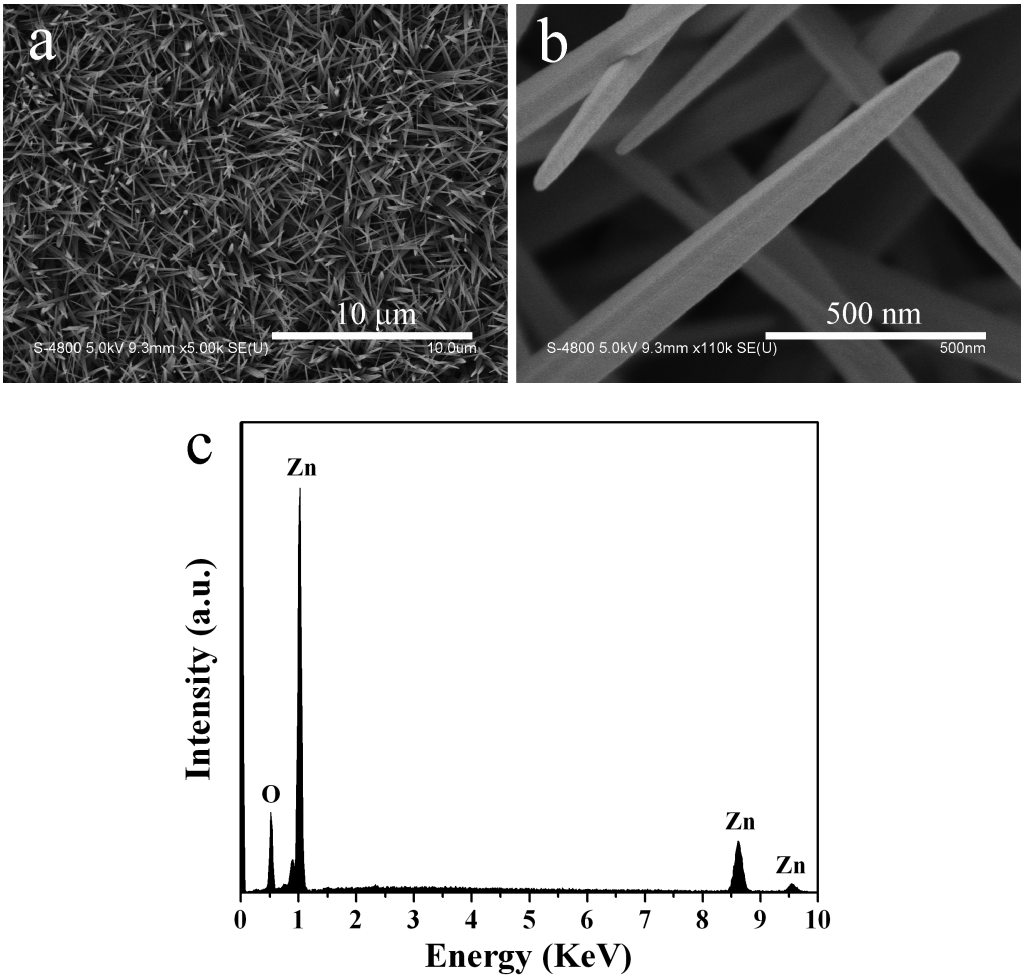

Fig. S2 Morphology and structural characterization of the ZnO-NRs. (a, b) Low and high magnification FESEM images, respectively, and (c) EDX spectrum.

A panoramic FESEM image in Fig. S2a clearly reveals that the ZnO sample is needle-like nanorods with several micrometers long and about 380 nm wide near the half height of the nanorods. The high magnification image in Fig. S2b shows the needle-like nanorods with smooth surfaces. The energy dispersive X-ray spectrum (Fig. S2c) shows the atomic ratio of Zn and O is 1:1, consistent with the stoichiometry of ZnO.

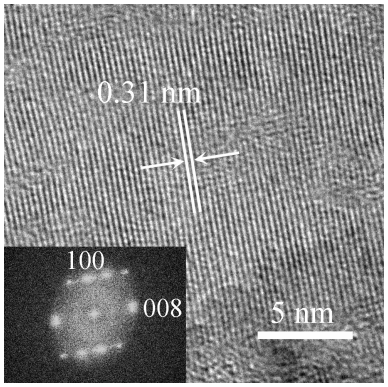

Fig. S3 HRTEM image obtained at the edge of the nanoplate. The inset is the corresponding fast Fourier transform (FFT) spot diagram. The lattice spacings of 0.31 nm correspond to (008) lattice planes of hexagonal ZnS with 8H symmetry.

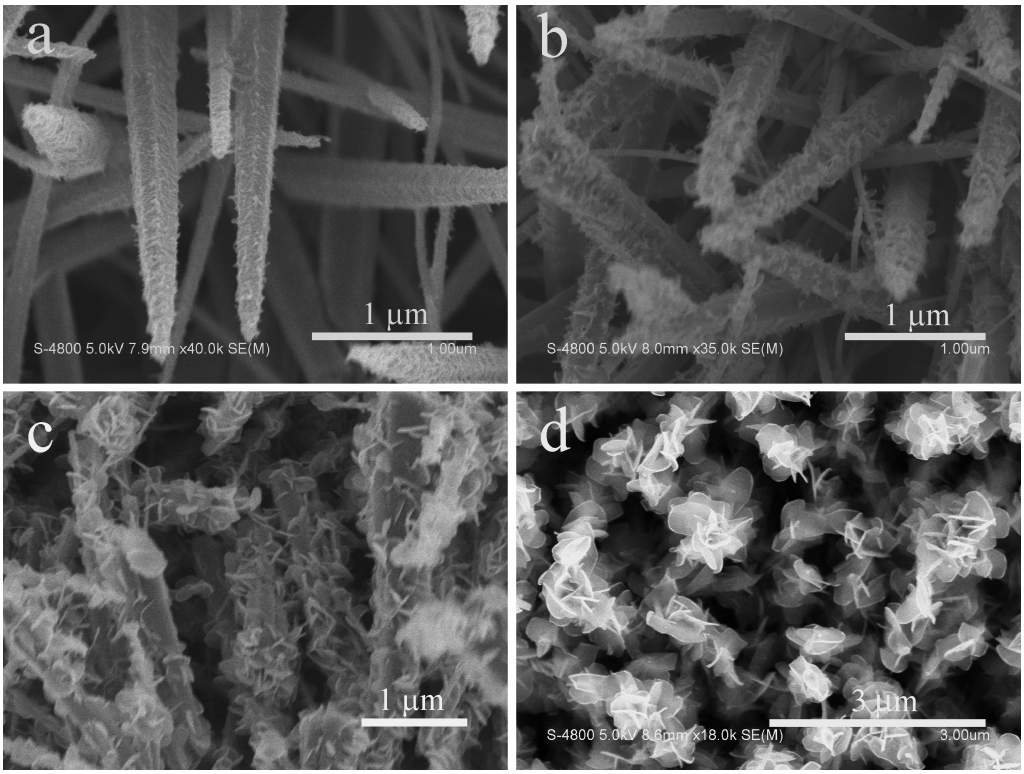

Fig. S4 Typical FESEM images of the ZnO-NRs/ZnS·$(HDA)_{0.5}$-NPs hierarchical heterostructure collected at different reaction times. (a) 10 min, (b) 30 min, (c) 60 min, and (d) 24 h.

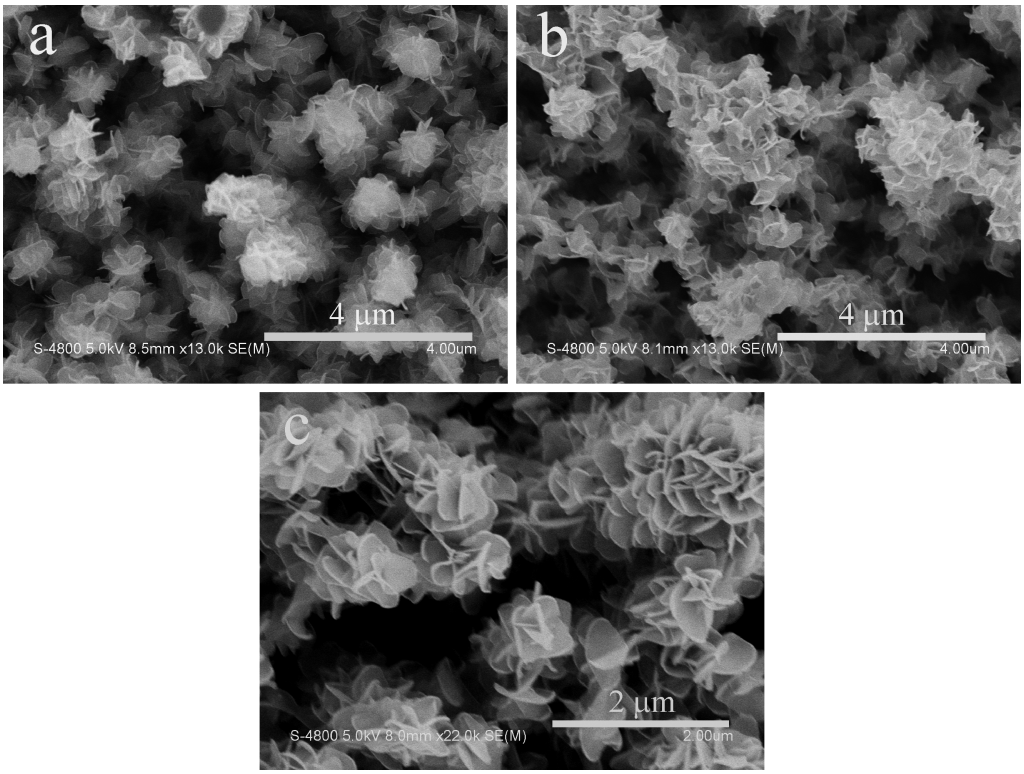

Fig. S5 FESEM images of the ZnO-NRs/ZnS·$(HDA)_{0.5}$-NPs hierarchical heterostructures synthesized under different concentrations of 1, 6-hexanediamin and Na_2S. (a) The product with 4 mL of 1, 6-hexanediamine, (b) The product with 6 mL of 1, 6-hexanediamine, and (c) The product with Na_2S concentration doubled.

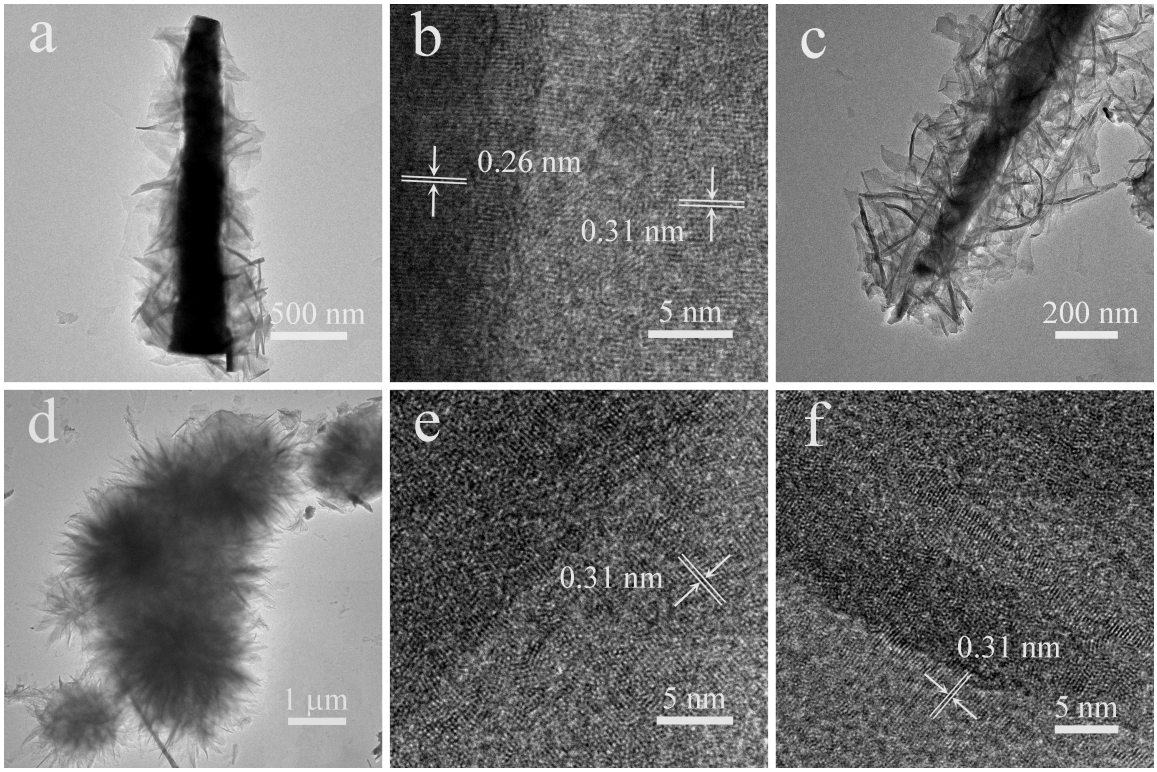

Fig. S6 TEM and HRTEM images of the products synthesized with other sulfur sources. (a) TEM image of a single ZnO-NRs/ZnS·$(HDA)_{0.5}$-NPs hierarchical heterostructure synthesized with thioacetamide as the sulfur source, (b) The corresponding HRTEM image of the junction, showing the single crystalline nature of the ZnO nanorod and ZnS nanoplate, (c) TEM images of a single ZnO-NRs/ZnS·$(HDA)_{0.5}$-NPs hierarchical heterostructure synthesized with thiosemicarbazideas as the sulfur source, (d) The corresponding top flowers dropped down by ultrasound treatment in sample preparation process for TEM observation, (e) HRTEM image of the junction shows the single crystalline nature of the ZnS nanoplate, and (f) HRTEM image taken from the top flower, also showing the single crystalline of ZnS.

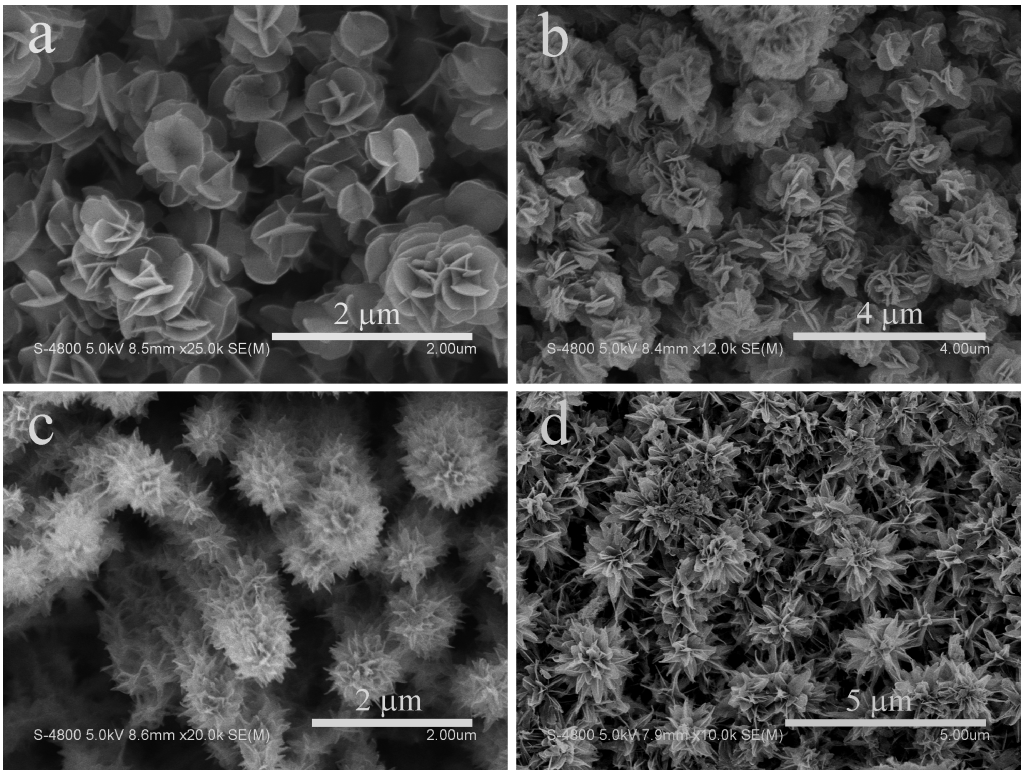

Fig. S7 FESEM images of the ZnO-NRs/ZnS·$(HDA)_{0.5}$-NPs hierarchical heterostructures synthesized under different concentrations of 1, 6-hexanediamin and the sulfur source. (a) The product with thioacetamide as the sulfur source with addition of 1 mL of 1, 6-hexanediamin, (b) The product with thioacetamide concentration doubled, (c) The product with thiosemicarbazide as the sulfur source with addition of 2 mL of 1, 6-hexanediamin, and (d) The product with thiosemicarbazide concentration doubled.

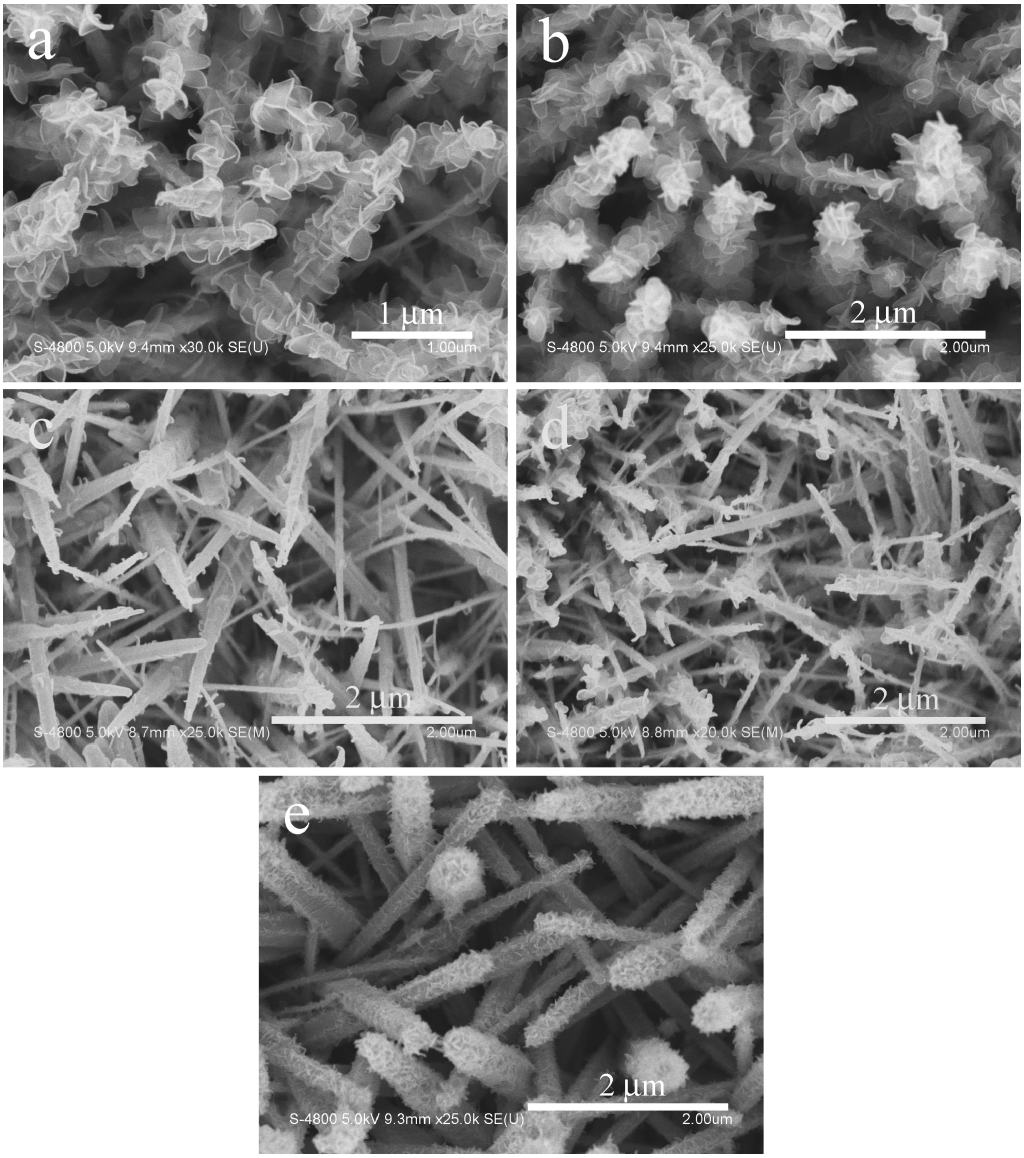

Fig. S8 FESEM images of the ZnO-NRs/ZnS·$(HDA)_{0.5}$-NPs heterostructures synthesized with varied temperature. (a) The product synthesized at 40°C with Na_2S as the sulfur source, (b) The product synthesized at 40°C with thioacetamide as the sulfur source, (c) The product synthesized at 20°C with Na_2S as the sulfur source, (d) The product synthesized at 20°C with thioacetamide as the sulfur source, and (e) The product synthesized at 100°C with thiosemicarbazide as the sulfur source.

The investigations of temperature on the microstructures of secondary hybrid ZnS nanoplates showed the ZnS·$(HDA)_{0.5}$-NPs with similar structure on ZnO-NRs were obtained at 40°C with Na_2S as the sulfur source (Fig. S8a), while thinner ZnS·$(HDA)_{0.5}$-NPs on ZnO-NRs at 40°C with

thioacetamide as the sulfur source (Fig. S8b). When the temperature was lower to 20°C, only few $ZnS{\cdot}(HDA)_{0.5}$-NPs covered on ZnO-NRs were gotten whether Na_2S or thioacetamide as the sulfur source (Fig. S8c and 8d, respectively.). When using thiosemicarbazide as the sulfur source, as the temperature was decreased to 100°C, only some tiny nanoplates covered on the nanorods were obtained (Fig. S8e).

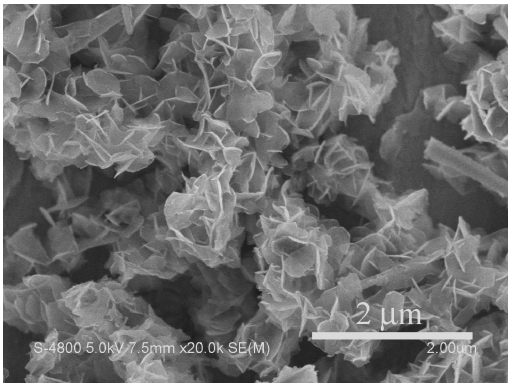

Fig. S9 FESEM image of the ZnO-NRs/ZnS·$(HDA)_{0.5}$-NPs product synthesized without the zinc substrate.

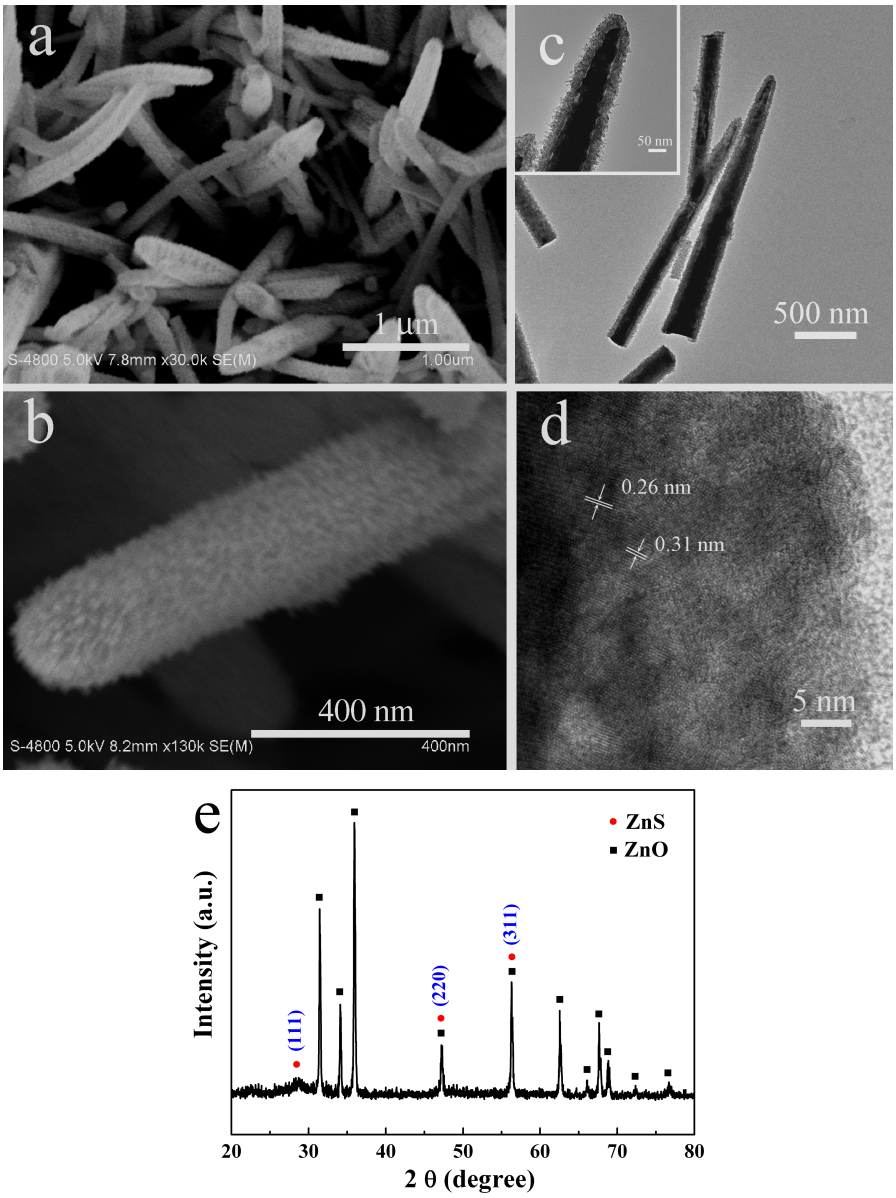

Fig. S10 Morphology and structural characterizations of the ZnO-NRs/ZnS nanoparticles heterostructure synthesized using $NH_3 \cdot H_2O$. (a, b) FESEM images at low and high magnifications, respectively, showing the product was nanoparticles covered on the ZnO-NRs, (c) TEM image of the product, further verifying the nanorods/nanoparticles core/shell structure. The inset clearly showed partially-dissolved ZnO core/ZnS shell nanostructure, (d) The HRTEM image of the heterostructure, showing the characteristic lattice planes of ZnO and ZnS as well as the polycrystalline nature of ZnS shell, and (e) The corresponding XRD pattern, demonstrating the product was ZnO and cubic ZnS (JCPDS No. 77-2100).

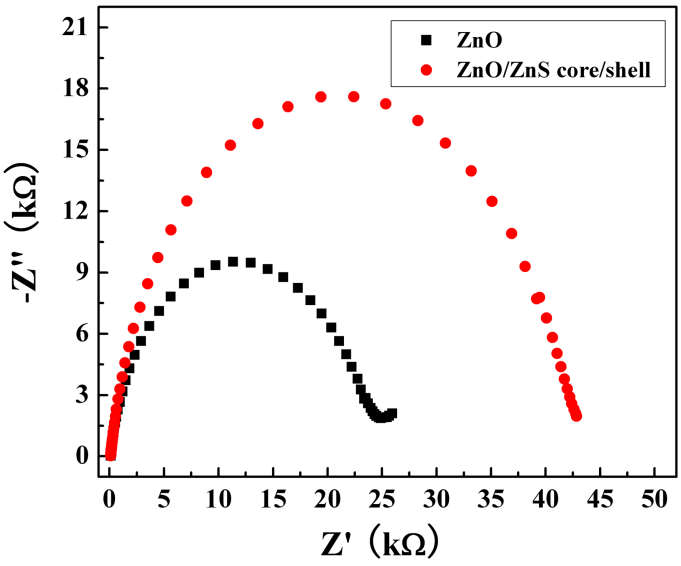

Fig. S11 Electrochemical impedance spectroscopy of the ZnO-NRs and ZnO-NRs/ZnS nanoparticles electrodes, which were obtained in 0.5 M KCl solution containing 5.0 mM $Fe(CN)_6^{3-}/Fe(CN)_6^{4-}$.